

Rapid #: -9573729

CROSS REF ID: **387214**

LENDER: **CSB :: Ejournals**

BORROWER: **LYU :: Main Library**

TYPE: Article CC:CCG

JOURNAL TITLE: Mechanisms of development

USER JOURNAL TITLE: Mechanisms of development

ARTICLE TITLE: Hsp47 mediates Cx43-dependent skeletal growth and patterning in the regenerating fin

ARTICLE AUTHOR: Bhadra, Joyita

VOLUME:

ISSUE:

MONTH:

YEAR: 2015

PAGES:

ISSN: 0925-4773

OCLC #:

Processed by RapidX: 8/20/2015 1:17:55 PM



This material may be protected by copyright law (Title 17 U.S. Code)



Contents lists available at ScienceDirect

Mechanisms of Development

journal homepage: www.elsevier.com/locate/mod

Hsp47 mediates Cx43-dependent skeletal growth and patterning in the regenerating fin[☆]

Joyita Bhadra, M. Kathryn Iovine*

Department of Biological Sciences, Lehigh University, United States

ARTICLE INFO

Article history:

Received 10 February 2015

Received in revised form 8 June 2015

Accepted 10 June 2015

Available online xxxx

Keywords:

Gap junction

Zebrafish

short fin

Joint formation

Cell proliferation

ABSTRACT

Skeletal morphogenesis describes how bones achieve their correct shape and size and appropriately position joints. We use the regenerating caudal fin of zebrafish to study this process. Our examination of the fin length mutant *short fin* (*sof^{b123}*) has revealed that the gap junction protein Cx43 is involved in skeletal morphogenesis by promoting cell proliferation and inhibiting joint formation, thereby coordinating skeletal growth and patterning. Here we demonstrate that *serpinh1b* is molecularly and functionally downstream of *cx43*. The gene *serpinh1b* codes for a protein called Hsp47, a molecular chaperone responsible for proper folding of procollagen molecules. Knockdown of Hsp47 in regenerating fins recapitulates the *sof^{b123}* phenotypes of reduced fin length, reduced segment length and reduced level of cell proliferation. Furthermore, Hsp47 knockdown affects the organization and localization of the collagen-based actinotrichia. Together, our findings reveal that *serpinh1b* acts in a *cx43* dependent manner to regulate cell proliferation and joint formation. We conclude that disruption of the collagen-based extracellular matrix influences signaling events required for cell proliferation, as well as the patterning of skeletal precursor cells that influences segment length. Therefore, we suggest that Hsp47 function is necessary for skeletal growth and patterning during fin regeneration.

© 2015 Elsevier Ireland Ltd. All rights reserved.

1. Introduction

Skeletal development in vertebrates is a tightly regulated process, although the underlying mechanisms that regulate the size and shape of bones remain largely unknown. Proper communication among cells of skeletal tissue is necessary in order to attain normal bone size and shape. One of the mechanisms by which cells communicate is through gap junctions, a group of channels between adjacent cells that allow the exchange of small molecules (<1000 Da), such as ions and second messengers (Goodenough et al., 1996). Each gap junction channel is formed by docking of two hemichannels from neighboring cells, and each hemichannel is composed of six connexin molecules. Connexins are proteins that are comprised of four transmembrane domains. In humans, there are approximately 21 different connexin genes (Sohl and Willecke, 2004). Among them, *CONNEXIN43* (*CX43*) is the most widely expressed connexin in bone cells (Jones et al., 1993). Gap junctional intercellular communication (GJIC) through Cx43 is of utmost importance during skeletal development. For example, mutations in human *CX43* cause oculodentodigital dysplasia (ODDD). ODDD is an autosomal dominant disease that causes craniofacial and

limb abnormalities (Flenniken et al., 2005; Paznekas et al., 2009). Mice lacking Cx43 die perinatally due to cardiac malformations (Reaume et al., 1995). However, examination of the neonatal bones of the *CX43* knockout mice reveals delayed ossification of axial and craniofacial skeletons (Lecanda et al., 2000). Additionally, targeted gene knockdown of Cx43 in chicks also causes ODDD-like phenotypes (McGonnell et al., 2001). In zebrafish, recessive mutations in *cx43* cause the *short fin* (*sof^{b123}*) phenotype, characterized by short fin length, short fin ray segments and reduced cell proliferation (Iovine et al., 2005). Together, these findings reveal that the role of Cx43 is conserved during skeletal development. However, how communication through GJIC brings about these tangible changes during skeletal development remains unclear.

We evaluate fin regeneration of the *sof^{b123}* mutant to provide insights into the role of Cx43 during skeletal morphogenesis. The *sof^{b123}* allele exhibits reduced levels of *cx43* mRNA and protein without a lesion in the coding sequence (Iovine et al., 2005; Hoptak-Solga et al., 2008). Importantly, morpholino-mediated knockdown of Cx43 in wild-type (WT) fins recapitulates all of the *sof^{b123}* phenotypes (Hoptak-Solga et al., 2008). In contrast to *sof^{b123}*, the *another long fin* (*alf^{dy86}*) mutant exhibits longer fins and stochastic joint failure (van Eeden et al., 1996). While the mutation is not in the *cx43* gene (Perathoner et al., 2014), this mutant shows an upregulation of *cx43* mRNA (Sims et al., 2009), suggesting that increased levels of *cx43* lead to joint failure. Indeed, Cx43 knockdown rescues joint formation in *alf^{dy86}*. Together, these gain-of-

[☆] NSF: IOS-1145582.

* Corresponding author at: 111 Research Drive, Iacocca B217, Bethlehem, PA 18015, United States. Tel.: +1 610 758 6981; fax: +1 610 758 4004.

E-mail address: mki3@lehigh.edu (M.K. Iovine).

function and the loss-of-function studies suggest that *cx43* is involved in skeletal morphogenesis in more than one way – by positively promoting cell proliferation and negatively regulating joint formation. Alternatively, one might speculate that reduced cell proliferation gives rise to shorter segments. However, it has been observed that reduced signaling via Shh or Fgfr1 dependent pathways cause reduced fin length and cell proliferation, but does not affect segment length (Quint et al., 2002; Lee et al., 2005). Therefore, cell proliferation is not sufficient to regulate segment length. We suggest that Cx43 coordinates skeletal growth (cell proliferation) and patterning (joint formation) during regeneration.

In order to address how Cx43 influences such tangible cellular outcomes like cell division and differentiation, we completed a microarray to identify downstream effectors of *cx43* that are downregulated in *sof*^{b123} and upregulated in *alf*^{dy86} (Ton and Iovine, 2012). Two genes have been validated through this microarray: *semaphorin3d* (Ton and Iovine, 2012) and *hapln1a* (Govindan and Iovine, 2014). Here we provide molecular and functional validation of a third gene, *serpinh1b*. The gene *serpinh1b* belongs to the serpin (serine protease inhibitor) family of proteases and codes for Hsp47 (Ishida and Nagata, 2011). Hsp47 is an ER resident protein that acts as a molecular chaperone for procollagen molecules, preventing their premature association into higher order collagen structure. Hsp47 binds to the procollagen triple helix in the pH-neutral ER and remains associated until reaching the Golgi, where the lower pH environment causes the procollagen to dissociate from Hsp47 (Nakai et al., 1992). Hsp47 is then recycled back to ER with the help of KDEL receptors (Satoh et al., 1996).

Recent studies have shown that autosomal recessive missense mutations in *SERPINH1* cause moderate to severe forms of Osteogenesis Imperfecta ('brittle bone' disease) in humans (Christiansen et al., 2010). The *SERPINH1* knockout mice does not survive beyond 11.5 days post coitus and displays abnormally oriented epithelial tissues and ruptured blood vessels due to severe deficiency in mature forms of type I and type IV collagen (Col) (Nagai et al., 2000). Chondrocyte specific knockout of Hsp47 causes severe chondrodysplasia and defective endochondral bone formation due to decreased level of type II and type XI Col (Masago et al., 2012). Therefore, Hsp47 function is critical for normal functions of collagen, including bone formation during skeletal development.

The teleost fin is supported by two types of skeletal elements – lepidotrichia and actinotrichia. The lepidotrichium is an individual bony fin ray composed of two hemirays of bone matrix which surrounds a mesenchyme consisting of fibroblasts, pigment cells, blood vessels and nerve cells. Several layers of epidermis surround the hemirays, where the basal layer of epidermis is the layer closest to the underlying lepidotrichium. Actinotrichia extend from the distal tips of growing fin rays during regeneration, providing a scaffold for migration for the osteoblast cells that will deposit the future bone matrix (Wood, 1982). Actinotrichia are produced by actinotrichia forming cells (AFC), located distally and immediately beneath the basal layer of the epidermis (Duran et al., 2011). The composition of actinotrichia includes elastoidin, which is a mix of collagen and non-collagenous proteins (Ramachandran, 1962; Sastry and Ramachandran, 1965). Recent studies have shown that the collagenous part of actinotrichia is composed mainly of Col I (expressed by the *col1a1a* gene) and Col II (expressed by the *col2a1b* gene (Duran et al., 2011)). The non-collagenous component of actinotrichia is composed of the proteins Actinodin-1 and Actinodin-2 (And1 and And2) (Zhang et al., 2010).

Here we demonstrate that *serpinh1b* is a *cx43*-dependent gene required for growth (cell proliferation) and patterning (joint formation) during skeletal morphogenesis. We find that the Collagen II dependent actinotrichia are disturbed following Hsp47 knockdown. We suggest that aberrant deposition of Collagen could influence both cell proliferation (through disturbing Integrin–Collagen interactions) and joint formation (through disturbing patterning of osteoblasts and joint-forming cells). These findings provide new insights into the roles of Hsp47 in the vertebrate skeleton.

2. Results

2.1. *serpinh1b* acts downstream of *cx43*

One of the candidate genes identified through the microarray was *serpinh1b*, which intrigued us due to the finding that mutations in human *SERPINH1* cause Osteogenesis Imperfecta (OI) (Christiansen et al., 2010). Hsp47 is the protein product of the gene *serpinh1b*. The zebrafish Hsp47 protein is 404 amino acids long and shares 64% sequence similarity with rat and mouse Hsp47, 69% with human Hsp47, and 72% with chicken Hsp47 (Pearson et al., 1996). In order to validate *serpinh1b* as a downstream target of *cx43*, we performed a whole mount in situ hybridization to compare the expression level of *serpinh1b* in WT, *sof*^{b123} and *alf*^{dy86}. As predicted, *serpinh1b* mRNA expression was upregulated in *alf*^{dy86} and downregulated in *sof*^{b123} (Fig. 1). Additional confirmation was provided by quantitative RT-PCR (qRT-PCR) to demonstrate reduced expression of *serpinh1b* in *sof*^{b123} and increased expression of *serpinh1b* in *alf*^{dy86} compared to WT (Fig. 2 and Supplementary Table 1). To further validate that *serpinh1b* expression is *cx43* dependent, we performed qRT-PCR on WT fins treated with *cx43* morpholino (MO). This is an independent test that *serpinh1b* expression depends on Cx43. Indeed, the expression level of *serpinh1b* is reduced following Cx43 knockdown (Fig. 2, Supplementary Table 1). Together, these data validate the microarray data and establish that *serpinh1b* is molecularly downstream of *cx43*.

In order to determine the tissue specific localization of *serpinh1b* mRNA, we performed in situ hybridization on cryosections of 5 days post amputation (dpa) regenerating fins. Longitudinal sections of the regenerating caudal fin are constituted of outer layers of epidermis separated from the mesenchyme by a layer of cuboidal cells known as basal layer of epidermis. A group of dedifferentiated cells occupy the distal end of the mesenchymal compartment and establish a specialized structure called the blastema. The blastema contains the proliferating cells required for fin outgrowth during regeneration. The skeletal precursor cells are the cells that differentiate as either osteoblasts or joint-forming cells, and are located laterally, between the actinotrichia and basal layer of epidermis (Ton and Iovine, 2013). The *serpinh1b* mRNA is most prominently expressed in the skeletal precursor cells, the overlying basal layer of epidermis, and in the blastema (Fig. 1D). These expression domains only partially overlap with Cx43 expression, which is found throughout the medial mesenchyme and in a discrete population of joint-forming cells in the lateral compartment (Hoptak-Solga et al., 2008; Sims et al., 2009). Therefore, we suggest that Cx43-dependent *serpinh1b* expression outside these domains requires an intermediate (such as a secreted growth factor) that acts between the medial mesenchyme and the lateral domains of *serpinh1b* expression (Ton and Iovine, 2012).

To determine how the expression pattern of *serpinh1b* changes during regeneration, we performed in situ hybridization on fins and on fin cryosections harvested at different timepoints (Fig. 3). We observed a similar pattern and similar levels of expression for 2.5, 3.5, 4 and 8 dpa regenerating fins by both whole mount in situ hybridization and in situ hybridization on cryosections. Staining of *serpinh1b* is not detected during ontogeny and is diminished at 14 dpa (Supplementary Fig. S1). Therefore, *serpinh1b* expression is upregulated during early stages of regeneration and is reduced in later stages of regeneration.

2.2. *serpinh1b* mediates downstream effects of *cx43*

In order to determine if *serpinh1b* mediates *cx43*-dependent growth and patterning, we evaluated regenerate length, cell proliferation and segment length following morpholino (MO) mediated gene knockdown. We used a gene specific MO targeting the start codon of *serpinh1b*. As a control, we used either a custom mismatch morpholino (5MM) containing five mismatches compared with the *serpinh1b*

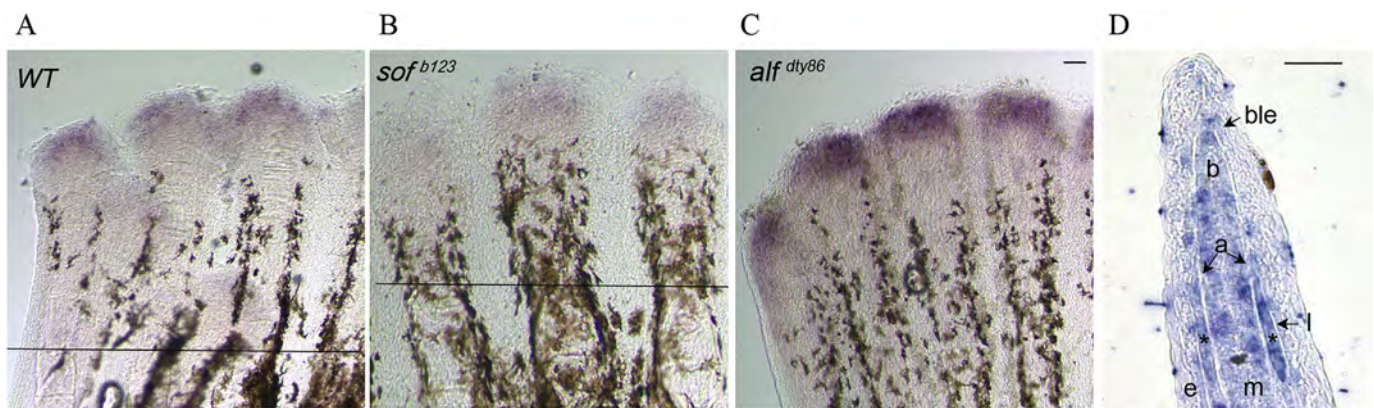


Fig. 1. *serpinh1b* is differentially expressed in wild-type, *sof*^{b123} and *alf*^{dy86}. Whole mount in situ hybridization shows increased expression in *alf*^{dy86} (C) and decreased expression in *sof*^{b123} (B) compared to wild-type (A). In situ hybridization on cryosection of a WT-5 dpa fin (D) reveals localization of *serpinh1b* in the blastema (b), basal layer of epidermis (ble) and skeletal precursor cells (*). Epidermis is denoted by 'e', mesenchyme by 'm', lepidotrichia by 'l' and actinotrichia by 'a'. The amputation plane is indicated in panels A and B. The amputation plane is beyond the field of view in C. The scale bars in C and D are 50 μ m; the scale bar in C applies to the images in A, B, and C.

targeting MO (Table 1), or a 'standard control' MO from Gene Tools that does not recognize any zebrafish genes. All MOs are modified with fluorescein, permitting evaluation of cellular uptake. Positive fins were harvested one day post electroporation (1 dpe) to evaluate cell proliferation and regenerate length, or fins were allowed to regenerate for four days (4 dpe) to measure segment length. Knockdown of Hsp47 was demonstrated by immunofluorescence (Fig. 4A) and by immunoblot (Fig. 4B) on MO positive fins, compared to control MO injected fins. Immunofluorescence on cryosections revealed the localization of Hsp47 protein in the regenerating fin. Hsp47 was observed in the basal layer of the epidermis as well as in the mesenchyme, similar to the expression pattern of the *serpinh1b* mRNA (Figs. 1 and 3). Quantification of Hsp47 protein expression from the immunoblot reveals an approximately 90% reduction following MO knockdown. Hsp47 levels in *sof*^{b123} and *alf*^{dy86} are affected as predicted. We find that *sof*^{b123} exhibits an approximately 25% decrease in expression level and that *alf*^{dy86} has an approximately 30% increase compared to WT (Fig. 4C). Differences in Hsp47 protein levels are therefore not as large in the

mutants as observed in the Hsp47 knockdown. However, since Hsp47 is a chaperone, the more permanent differences in Hsp47 function of the mutants may have a stronger impact on collagen structure.

To evaluate the phenotypic effects following knockdown of Hsp47, we compared the target or control MO injected side with the respective uninjected side and calculated the percent similarity. Values with high similarity between the injected and noninjected side (i.e. close to 100%) indicate little effect of the MO, whereas values with low similarity (i.e. less than 100%) indicates that the MO had an effect on treatment side. This method minimizes fin-to-fin variation since the uninjected side serves as an internal control for each fin. We first evaluated changes in outgrowth, which are measured by regenerate length and cell proliferation. Fin length was measured as the distance between the amputation plane and the distal end of the regenerate. The level of cell proliferation was measured by counting cells in mitosis, labeled with an antibody against histone 3 phosphate (H3P). When using the control MO, we found high similarity between the treatment and control sides for regenerate length and cell proliferation, revealing no effect. In contrast, Hsp47 knockdown with the targeting MO exhibited reduced levels of similarity for cell proliferation and regenerate length; cell proliferation is approximately 25% reduced (Fig. 5C) and regenerate length is about 20% reduced (Fig. 5F). We next evaluated segment length, measured in calcein stained fins as the distance between the first two joints distal to the amputation plane. We found that segment length was about 10% reduced when using the targeting MO, and was not reduced when using the control MO (Fig. 6A,C). Since Hsp47 knockdown has a milder effect on segment length, it may not play a major role in regulating joint formation. In summary, we find that Hsp47 knockdown recapitulates all Cx43-knockdown phenotypes indicating that *serpinh1b* is functionally downstream of *cx43*.

Since Hsp47 is a collagen chaperone, we further evaluated the length of regenerated bone matrix. This was measured as the distance between the amputation plane and the tip of the calcein stained bone matrix, and was normalized against the total regenerate length. Following Hsp47 knockdown, we found a small but significant difference in the bone regenerate length, about 4% reduced (Fig. 6A,D). This finding suggests that bone-forming cells can secrete matrix. The quality of the secreted bone matrix in Hsp47 knockdown fins will be evaluated in future studies.

Since mutations in *serpinh1b* gene are associated with a recessive form of OI, we tested whether the short segment phenotype was caused by breaks in bone matrix (i.e. caused by brittle lepidotrichia) or due to formation of premature joints (i.e. caused by differences in skeletal patterning). ZNS5 staining identifies both joint-forming cells and osteoblasts, and can be used to distinguish these possibilities (Sims et al., 2009). We observed ZNS5 positive cells around the joints (Fig. 7),

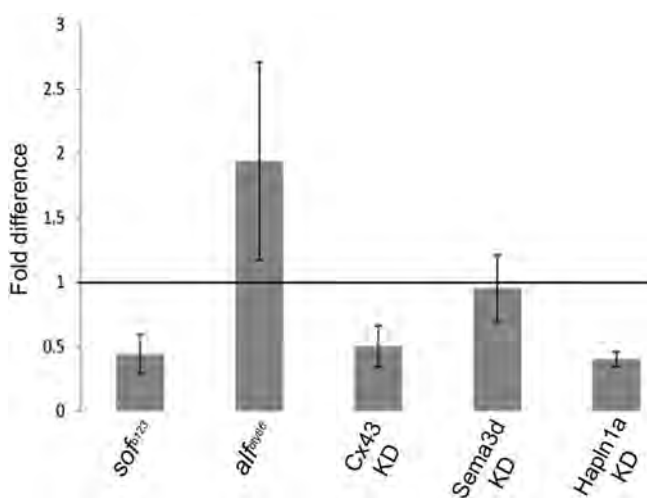


Fig. 2. Changes in *serpinh1b* expression by quantitative RT-PCR. Expression of *serpinh1b* is down-regulated in *sof*^{b123} and upregulated in *alf*^{dy86} when compared to WT. *serpinh1b* expression level decreases following Cx43 and Hapln1a knockdown and remains unchanged following Sema3d knockdown when compared to standard control MO injected fins. The error bars represent the range in variation of the fold-difference based on the standard deviation. A fold-difference of one indicates no change in expression between experimental and control samples.

Table 1
Primers and morpholinos.

Genes	Primers for ISH	Primers for qRT-PCR	Morpholinos
<i>serpinh1b</i>	F = ATGTGGTATCCAGCCTC RT7 = TAATACGACTCACTATA GGGTACCCCTTAGGCGAACTAGCC	F = AGGATGTGAAAAACACAGACG R = TGGAACTTCTCATCCAGTGG	MO = GCAATGAGGCT GGATACCCACATTC 5MM = GCATcAGcCTGcATAgCCACATTC
<i>msxb</i>		F = GACCCGTGAAACGACATCT R = GCCATCAGGGATTCAACT	
<i>msxc</i>		F = CAACCTCTCCGACTGCAAGAGA R = TGAATGCCTTGGCGGAGAA	
<i>mps1</i>		F = TTCAAGTCTCCGCTCTGCA R = TCTGGACTGATAACAGGTGGCT	

The T7 RNA polymerase binding site in the reverse primer is in bold. F = forward primer, RT7 = reverse primer, MO = targeting morpholino, 5MM = control morpholino with 5 mismatch pairs to target sequence. All primers and MOs are shown in 5' to 3' orientation.

revealing that shorter segments were caused by formation of premature joints and not by breaks in the matrix (which would not be associated with ZNS5 positive cells).

In order to confirm that markers of cell proliferation are reduced following Hsp47 knockdown, we evaluated expression levels of the transcription factors *msxb* and *msxc*, and the intracellular kinase *mps1*. These genes are expressed in the blastema during regeneration and have been found to be required during cell proliferation (Akimenko et al., 1995; Nechiporuk and Keating, 2002; Poss et al., 2002; Smith et al., 2006; Thummel et al., 2006). Interestingly, knockdown of Hsp47 in WT 5 dpa fins resulted in reduced *msxb* and *msxc* expression, whereas the expression level of *mps1* remain unaffected (Fig. 8 and Supplementary Table 2). This finding supports the conclusion that cell proliferation is reduced following Hsp47 knockdown.

2.3. Role of *serpinh1b* on collagen structure

Hsp47 functions as a molecular chaperone for collagen by binding to the procollagen triple helix in ER. This interaction is believed to prevent

premature higher order aggregation of procollagen (Widmer et al., 2012; Eyre and Weis, 2013). In order to determine if Hsp47 influences collagen assembly and/or organization during fin regeneration, we evaluated the localization of Col II, a major component of actinotrichia following Hsp47 knockdown. In longitudinal sections of WT 5 dpa regenerating fins, Col II was observed prominently in the actinotrichia in its characteristic fibrillary pattern (Fig. 9). As part of these studies, we realized that injections with standard control MO (Fig. 10) or DMSO (data not shown) altered the longitudinal fibrillar structure of actinotrichia in a time-specific manner. The fibrillar association is disrupted immediately following injection, and recovers by 3–4 days post injection. In contrast, we did not observe changes in actinotrichia in transverse sections following either control treatment (Fig. 10 for standard control MO; data not shown for DMSO control). As soon as one day post injection in transverse sections, actinotrichia are observed appropriately in two symmetric rows beneath the epidermis. Therefore, for continued functional studies we evaluated transverse sections. We also note that the antigen retrieval protocol used for immunofluorescence completely eliminated the fluorescein from the MO

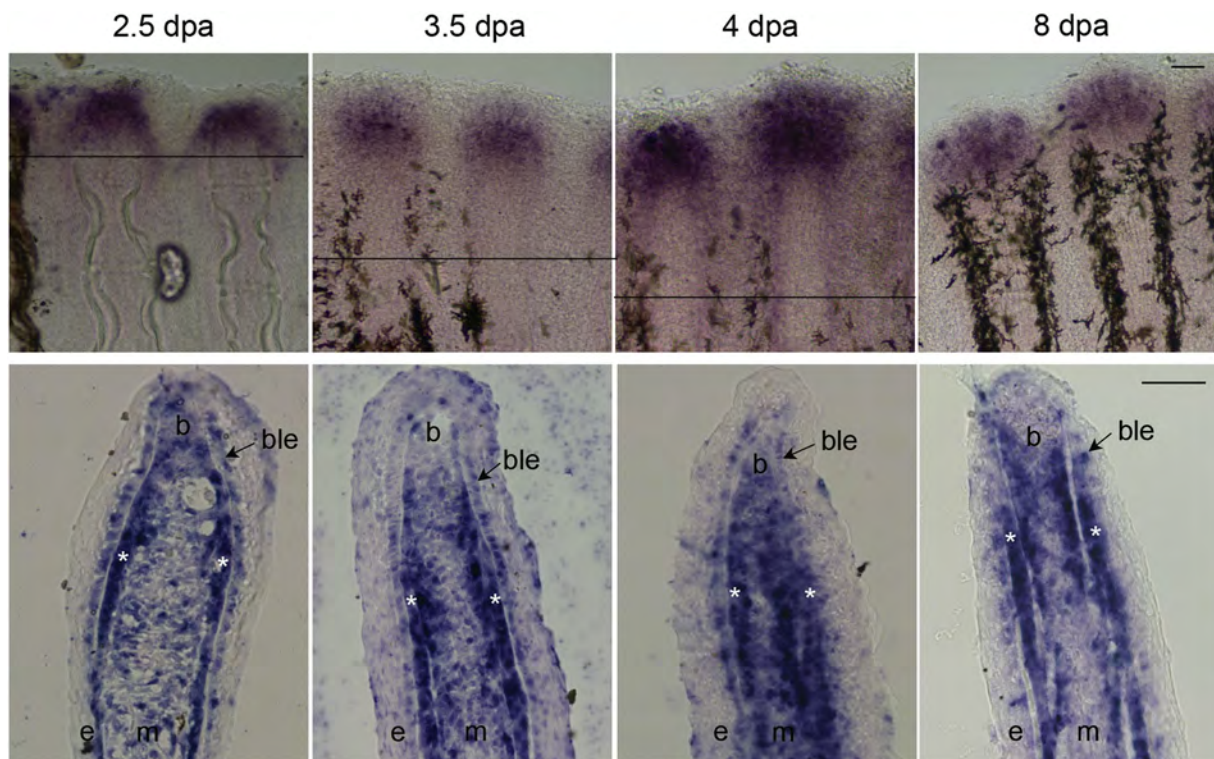


Fig. 3. *serpinh1b* expression over time in regenerating fins. Whole mount in situ hybridization for *serpinh1b* at different time points on regenerating fins (top). The amputation plane is indicated in 2.5, 3.5 and 4 dpa fins. For 8 dpa fins, the amputation plane is outside the field of view. In situ hybridization on cryosectioned fins at different time points (bottom). Similar localization of *serpinh1b* gene in basal layer of epithelium (ble) and skeletal precursor cells (*) is observed. Blastema (b), basal layer of epidermis (ble), and skeletal precursor cells (*). The scale bars are 50 μ m. The scale bar in the upper 8 dpa panel applies to all panels for whole mount images. The scale bar in the lower 8 dpa panel applies to all panels for cryosections.

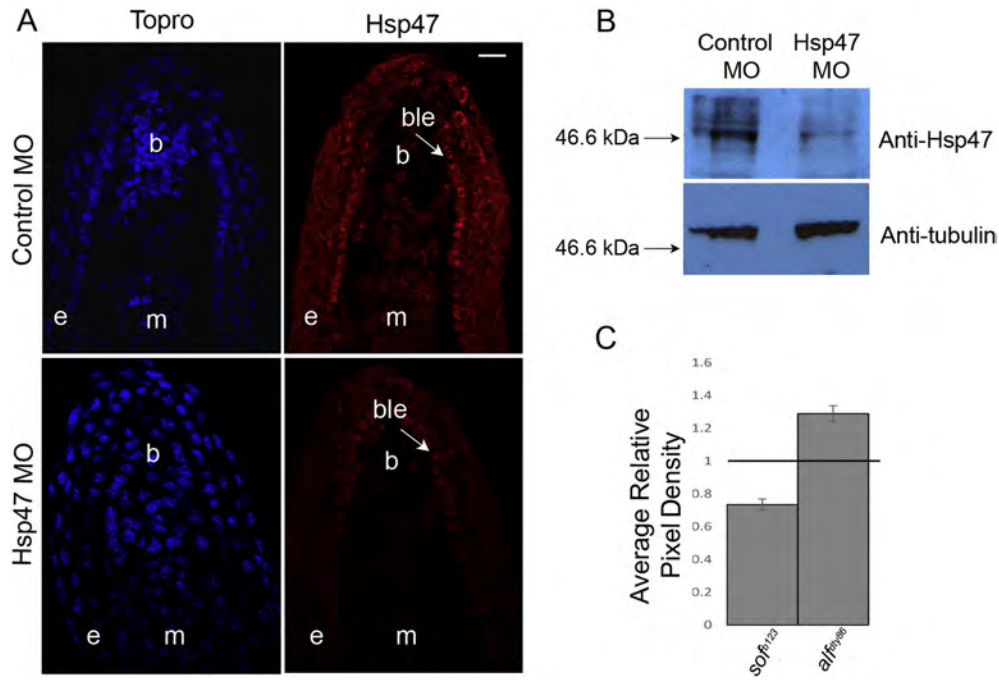


Fig. 4. Morpholino mediated knockdown of Hsp47 results in reduced expression in WT regenerating fins. (A) Longitudinal sections of WT 5 dpa fins following treatment with standard control or targeting MO against *serpinh1b*. Hsp47-MO treated fins show reduced level of Hsp47 expression. Hsp47 (red), nuclei are stained with the far red dye To-Pro (blue). 'ble' indicates basal layer of epithelium; 'b' blastema; 'm' mesenchyme, and 'e' epidermis. Scale bar is 10 μ m, and applies to all panels in A. (B) Immunoblots confirming reduced level of Hsp47 following Hsp47 knockdown. Hsp47-MO treated fins (MO) are compared to fins injected with standard control MO. Tubulin is used as loading control. (C) Bar graph depicting the ImageJ analysis of the ratio of Hsp47 levels between *sof^{b123}* or *alf^{dy86}* and wild-type (normalized by the tubulin loading control). Hsp47 protein levels are reduced in *sof^{b123}* and upregulated in *alf^{dy86}* relative to WT (represented as a relative density of 1).

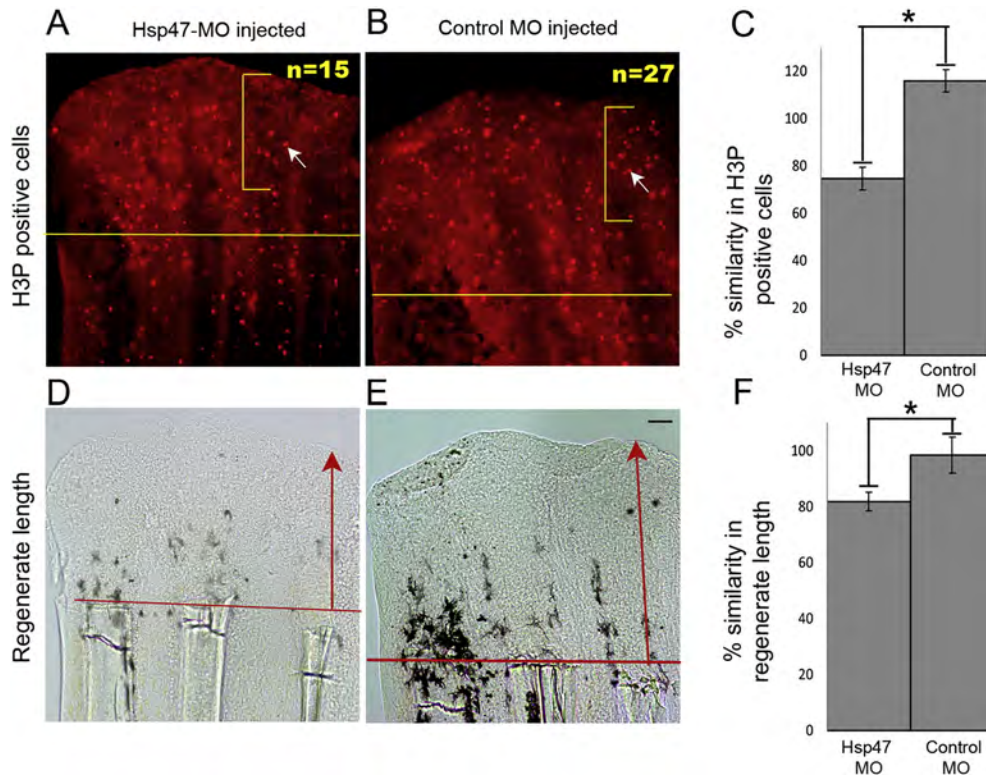


Fig. 5. Morpholino mediated knockdown of Hsp47 causes reduced cell proliferation and fin length. All fins were amputated at the 50% level prior to injection and electroporation. Fin rays treated with targeting or control MO (injected) were measured and compared to their uninjected sides. The ratio of the injected side (targeting MO or control MO) and the control uninjected side, multiplied by 100, is the percent similarity. Percent similarity of greater than 100% reflects the fact that the experimental side can be measurably larger than the control uninjected side. (A–C) Total number of H3P positive cells (white arrows identify one positive cell in each panel) were counted in injected and uninjected sides for Hsp47-MO (A) and Hsp47-5MM (B) treated fins. (C) The bar graph shows reduced level of H3P positive cells in Hsp47 MO injected fins compared to the control MO. (D–F) Total regenerate length in Hsp47-MO (D) and Hsp47-5MM (E) injected fins was measured by evaluating the distance between the distal tip of the fin and the amputation plane (indicated by red arrows) and normalized to the respective uninjected side. (F) Bar graph shows reduced regenerate length in Hsp47 MO treated fins. Scale bar is 50 μ m and applies to all panels. The student's *t*-test was performed ($p < 0.05$) to determine significance.

and therefore did not interfere with the immunofluorescence in the 488 channel (data not shown).

Following standard control MO treatment Col II is localized in the two well-organized symmetric rows of actinotrichia (Figs. 10 and 11A). Strikingly, the organization of the actinotrichia is severely disrupted following Hsp47 knockdown (Fig. 11A). The two well-organized rows of actinotrichia are lost. Some rods of actinotrichia may be present, but are much smaller in diameter than actinotrichia from the control fins. To provide further evidence that Hsp47 functions in a common pathway with Cx43, we next evaluated actinotrichia in Cx43 knockdown, and in *sof*^{b123} and *alf*^{dy86} 5 dpa regenerating fins. Fins treated for Cx43 knockdown exhibited similar disruptions of actinotrichia as were

observed for Hsp47 knockdown (Fig. 11A). In the *sof*^{b123} and *alf*^{dy86} mutants, we observed variability in the severity of the actinotrichia morphology. We categorized the phenotypes as “mild,” where the overall organization into two rows of actinotrichia is maintained but the individual actinotrichia may appear smaller; “disrupted,” where the organization of actinotrichia into two discrete rows is not maintained; and “small,” where there are more obvious reductions in the size of the actinotrichia (Fig. 11B). Actinotrichia in *sof*^{b123} mutants were generally much smaller in diameter and were sometimes disorganized. Actinotrichia in *alf*^{dy86} were often both smaller and disorganized. Thus, the phenotypes of Cx43 knockdown, *sof*^{b123}, and *alf*^{dy86} are consistent with defects in Collagen maturation, and are similar with what is observed for Hsp47 knockdown. These findings provide further support for the hypothesis that *cx43* and *serpinh1b* function in a common molecular pathway.

2.4. *serpinh1b* functions in the *cx43*-*hapln1a* dependent pathway

Prior studies have validated both *sema3d* and *hapln1a* as downstream effectors of *cx43* (Ton and Iovine, 2012; Govindan and Iovine, 2014) contributing to promotion of cell proliferation and inhibition of joint formation. As part of those studies, it was determined that neither *sema3d* nor *hapln1a* depend on each other for their transcription. Therefore, it was suggested that the *sema3d* and *hapln1a* molecular pathways act independently of each other (Govindan and Iovine, 2014). In order to evaluate whether the transcription of *serpinh1b* is dependent on either *sema3d* or *hapln1a*, we evaluated *serpinh1b* expression following knockdown of *Sema3d* or *Hapln1a*. We find that expression of *serpinh1b* is reduced following *Hapln1a* knockdown, but not following *Sema3d* knockdown (Fig. 2 and Supplementary Table 1). These findings suggest that *serpinh1b* is transcriptionally downstream of *hapln1a* but not *sema3d* (Fig. 12A).

3. Discussion

Here we demonstrate that *serpinh1b* is molecularly and functionally downstream of *cx43*. We observe that the expression of *serpinh1b* is reduced in *sof*^{b123}, elevated in *alf*^{dy86}, and that Cx43 knockdown reduces *serpinh1b* expression. Further, we find that Hsp47 knockdown recapitulates the *cx43*-dependent phenotypes, namely reduced regenerate length, reduced segment length and a reduced level of cell proliferation. Moreover, we find that Hsp47 knockdown and changes in Cx43 activity lead to similar defects to actinotrichia, the collagen-based rods produced at the growing end of the fin. Together, these findings provide strong support for the hypothesis that *serpinh1b* functions in a common pathway with *cx43*. Since this is the third gene identified from a microarray to identify *cx43*-dependent genes, we also placed *serpinh1b* in the *cx43*-dependent gene network downstream of *hapln1a* (Fig. 12A).

The *serpinh1b* gene codes for the collagen chaperone Hsp47. Hsp47 resides in the ER and binds procollagen trimers in order to prevent aggregation within the secretory pathway (Widmer et al., 2012; Eyre and Weis, 2013). Once procollagen trimers are secreted, they are processed to mature forms and assembled into fibers. Remarkably, a recessive mutation in human *SERPINH1* causes a severe form of brittle bone disease, OI, due to unstable type I Collagen (Christiansen et al., 2010). Moreover, knockout of *SERPINH1* in mice is embryonically lethal due to defective type I and type IV Collagen (Nagai et al., 2000). Chondrocyte-specific knockout of *SERPINH1* causes substantially reduced secretion of type II and type XI Collagen in cartilage, resulting in faulty endochondral bone formation (Masago et al., 2012). Therefore, the function of Hsp47 is critical for collagenous structures, and in particular in the formation of bone matrix.

Mutations in two collagen genes have been found to influence collagen-based structures in the regenerating fin. Mutations in the *col9a1* gene (causing the *persistant plexus/prp* phenotypes) lead to

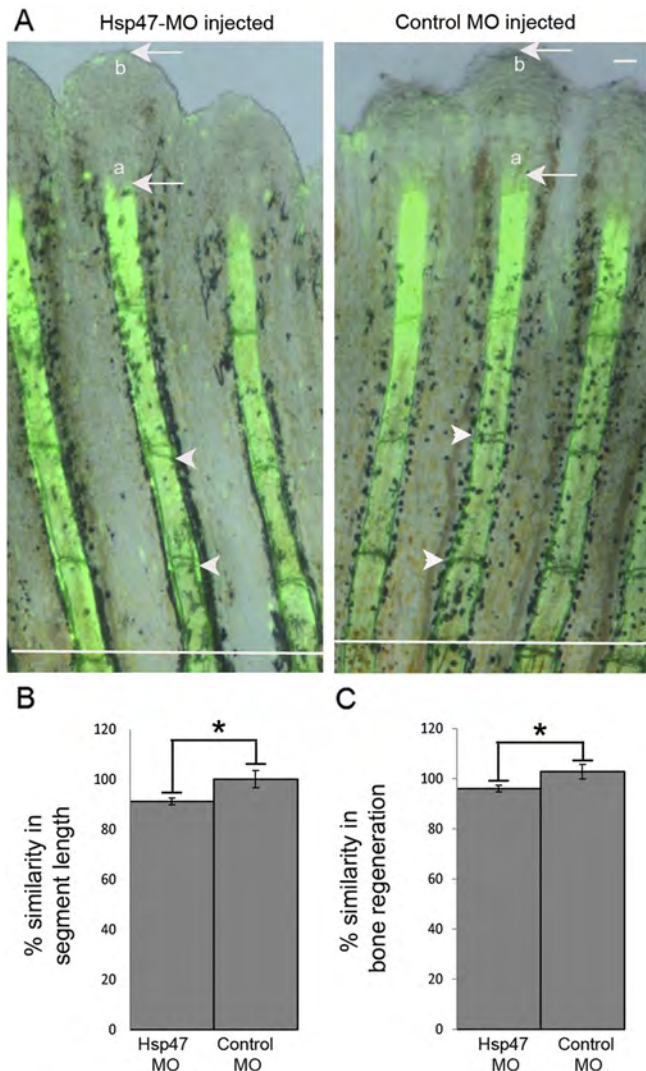


Fig. 6. Morpholino mediated knockdown of Hsp47 causes reduced segment length and a small change in bone regenerate length. Calcein staining was used to measure segment length and bone regenerate length in the regenerate. The amputation plane is indicated by a white line. Fin rays treated with targeting or control MO (injected) were measured and compared to their uninjected sides. The ratio of the injected side (targeting MO or control MO) and the control uninjected side, multiplied by 100, is the percent similarity. Percent similarity of greater than 100% reflects the fact that the experimental side can be measurably larger than the control uninjected side. (A) Segment length in Hsp47-MO and Hsp47-5MM injected fins was measured as the distance between the 1st and the 2nd joints (indicated by white arrow heads) distal to the amputation plane. Bone regenerate length was measured as the ratio of the distance of the regenerated length of the calcein stained bone matrix (marked as a) and the total regenerate length (marked as b). The treatment side was normalized against the uninjected side. (B) Bar graph shows reduced segment length following Hsp47 MO injection ($p < 0.05$). (C) Bar graph shows small but significant reduction in bone regenerate length. The scale bar is 50 μ m and applies to both panels in A. The student's *t*-test was performed ($p < 0.05$) to determine significance.

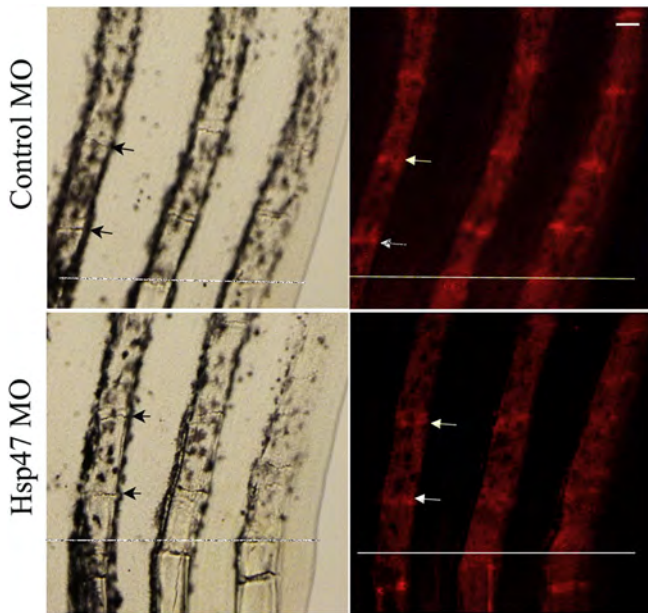


Fig. 7. The short segment phenotype following Hsp47-MO treatment is due to formation of premature joints. ZNS5 immunostaining detects osteoblasts and joint-forming cells. Brightfield (left) and ZNS5 immunostaining (right) images are shown. ZNS5 positive joints (indicated by arrows) are observed in both standard control (top row) and targeting MO (bottom row) treated fins. Scale bar is 50 μ m and applies to all panels.

disintegration of the actinotrichia and mispatterning of the osteoblasts that secrete the bony matrix of the lepidotrichia (Huang et al., 2009). The resulting lepidotrichia exhibit a wavy appearance, in stark contrast to straight wild-type fin rays. The Col IX protein serves to cross-link the fibrillar Col II (Diab et al., 1996), and may be responsible for the integrity of Col II fibrils. Mutations in the *col1a1a* gene cause the *chihuahua/chi* phenotypes, (Fisher et al., 2003) and lead to stochastic failure of actinotrichia formation in the regenerating fin (Duran et al., 2011). Fin rays without actinotrichia exhibit a wavy appearance, while fin rays that produce actinotrichia are straight. Col I was identified as a component of the actinotrichia following proteomic analyses, although it remains uncertain how Col I and Col II interact to form fibrils (Duran et al., 2011). Defects in these collagen proteins likely have a direct impact on the structure of actinotrichia, but it is unknown if the concomitant effects on lepidotrichia are direct or indirect. Since Hsp47

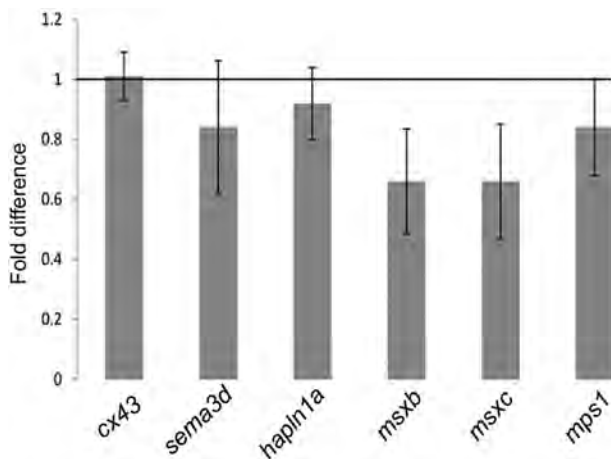


Fig. 8. Identifying changes in gene expression following Hsp47 knockdown using qRT-PCR. Expression level of *msxb* and *msxc* decreases following Hsp47 knockdown. No change is observed in the expression levels of *cx43*, *sema3d*, *hapln1a* and *mps1*. Hsp47 knockdown samples are compared to standard control MO treated samples. The error bars represent the range in variation of the fold-difference based on the standard deviation. A fold-difference of one indicates no change in expression between experimental and control samples.

is a collagen chaperone, it is not surprising that we also observe defects in actinotrichia following Hsp47 knockdown.

We focused on Col II in our studies to identify the effects of Hsp47 knockdown. We find that the structure of actinotrichia is highly perturbed following changes in Hsp47 expression in the regenerating fin, not unlike the appearance of the actinotrichia of the Col9a1 knockdown (Huang et al., 2009). It is not known how changes in the size and organization of the actinotrichia impact the Cx43 phenotypes of reduced cell proliferation and joint formation. However, the actinotrichia are located directly adjacent to both the proliferating cells of the blastema and to the skeletal precursor cells. Therefore, one possibility is that the Col II in the actinotrichia signal to the cells of both compartments (Fig. 12B). For example, Integrins can serve as collagen receptors and transduce outside-in signaling that may influence changes in gene expression (Heino, 2014). Thus, one possibility is that Hsp47-dependent cell proliferation is the result of aberrant Collagen-Integrin interactions, which could in turn influence the expression levels of genes required for cell proliferation. Similarly, Hsp47-dependent segment length may be the result of defective actinotrichia signaling inappropriate differentiation of osteoblasts and/or joint-forming cells. In turn, this may lead to the observed short segment phenotype in Hsp47-knockdown fins. Indeed, the *col9a1/prp* mutant exhibits both mispatterning of osteoblasts and short segments (Huang et al., 2009).

This study builds on our model of *cx43*-dependent gene interactions by validating a third gene identified in our microarray analysis. We not only demonstrate that *serpinh1b* is molecularly and functionally downstream of *cx43* and *hapln1a*, but we also extend the function of Hsp47 by demonstrating that Hsp47 can influence bone growth and skeletal patterning. Hsp47 is believed to exert its function through the organization of Collagen proteins in the extracellular matrix. Future studies will further elucidate mechanistically how Collagen structure impacts cell proliferation and joint-formation.

4. Experimental procedures

4.1. Statement on the ethical treatment of animals

This study was carried out in strict accordance with the recommendations provided by the National Institute of Health in the Guide for the Care and Use of Laboratory animals. The protocols used for this manuscript were approved by Lehigh University's Institutional Animal Care and Use Committee (IACUC) (protocol identification # 128, approved on 11/16/2014). Lehigh University's Animal Welfare Assurance Number is A-3877-01. All experiments were designed to minimize pain and discomfort to the animals.

4.2. Housing and husbandry

Zebrafish are housed in a recirculating system built by Aquatic Habitats (now Pentair). Both 3 L tanks (up to 12 fish/tank) and 10 L tanks (up to 30 fish/tank) are used. The fishroom has a 14:10 light:dark cycle and room temperature varies from 27–29 °C (Westerfield, 1993). Water quality is automatically monitored and dosed to maintain conductivity (400–600 μ S) and pH (6.95–7.30). Nitrogen levels are maintained by a biofilter. A 10% water change occurs daily. Recirculating water is filtered sequentially through pad filters, bag filters, and a carbon canister before circulating over UV lights for sterilization. Fish are fed three times daily, once with brine shrimp (hatched from INVE artemia cysts) and twice with flake food (Aquatox AX5) supplemented with 7.5% micropellets (Hikari), 7.5% Golden Pearl (300–500 μ , Brine Shrimp direct), and 5% Cyclo-peeze (Argent).

4.3. In situ hybridization (ISH) on whole mount and cryosectioned fins

Antisense *serpinh1b* probe was generated from 250–500 ng of PCR amplified linear DNA in which the reverse primer contained the binding

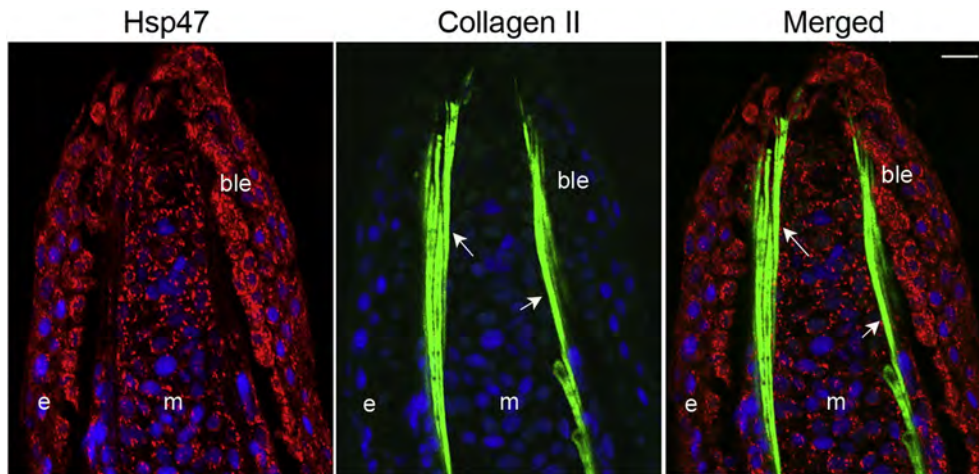


Fig. 9. Localization of Hsp47 and Collagen type II in WT-5 dpa fins. Confocal images of a WT-5 dpa longitudinal fin section immunostained with Hsp47 (red) and collagen type II (green) and counterstained with To-pro to detect nuclei (blue). Arrows indicate actinotrichia. 'ble' is basal layer of epithelium, 'e' epidermis and 'm' mesenchyme. Scale bar is 10 μ m and applies to all panels.

site for T7 RNA polymerase. The primer sequences for ISH is presented in Table 1. In situ hybridization on whole mount regenerating and cryosectioned fins was performed following standard protocols (Ton and Iovine, 2012; Govindan and Iovine, 2014).

4.4. Morpholino mediated knockdown in regenerating fins

All fins were amputated at the 50% level. Morpholinos (MO) used for this study were obtained from Gene Tools, LLC and were fluorescently tagged (Table 1). The working concentration was 1 mM. The targeting MO blocks the ATG. Two different control MO were used – the standard control MO from Gene Tools or the five nucleotide mismatch MO. MOs were injected in half the fin at 3 dpa followed by electroporation for cellular uptake (injection and electroporation was carried out as described) (Ton and Iovine, 2012). Fins were evaluated for uptake at 1 dpe (days post electroporation). For histone-3-phosphate (H3P) staining and qRT-PCR analysis, fins were harvested 1 dpe. For calcein

staining or ZNS5 staining, fins were harvested at 4 dpe. Each MO knockdown was carried out in at least three independent experiments with $n = 7-10$. Statistical significance was determined using Student's t -test ($p < 0.05$).

4.5. Lysate preparation and western blotting

Approximately 10–15 fins were injected with target or control MO on 3 dpa and harvested the next day. For measuring antibody staining in WT, *sof*^{b123} and *alf*^{dy86} fins, approximately 10–12 WT fins, 20 *sof*^{b123} fins and 8–10 *alf*^{dy86} fins were harvested at 5 dpa. Regenerating fins were harvested in 300–500 μ l of Incubation buffer (pH = 7.5) supplemented with 200 μ M Pefabloc, 1 mM DTT and protease inhibitor (Thermo Scientific, Halt™ protease and phosphatase inhibitor cocktail). Fins were homogenized using a tissue homogenizer (Bio-Gen, PRO 200) at high speed (5 \times) for 5 s with a 10 s cooling time in between. Homogenized samples were centrifuged at 200 g for

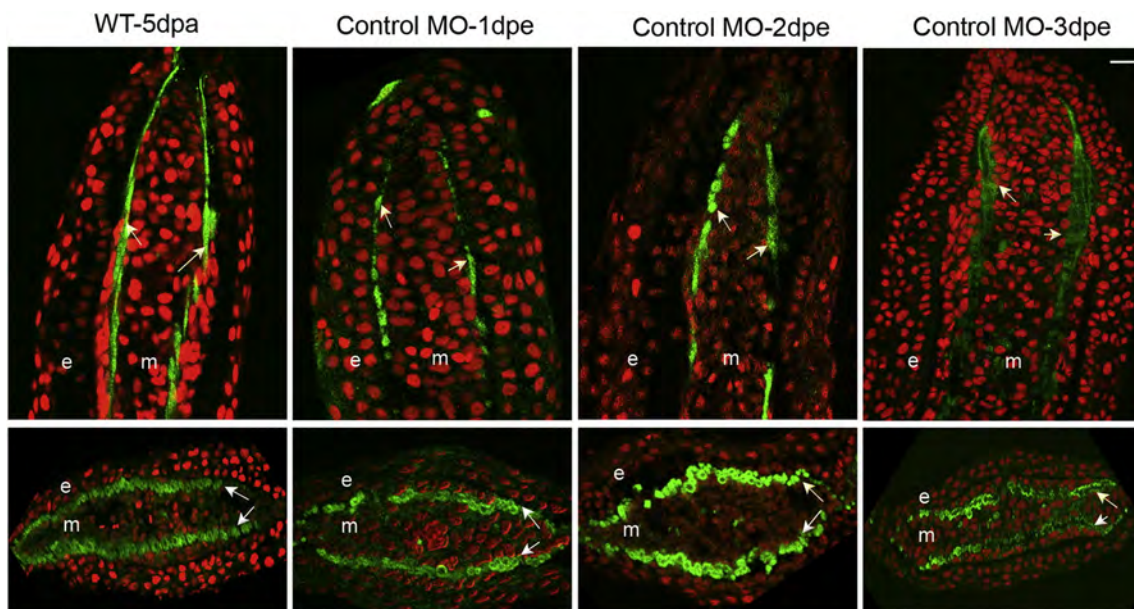


Fig. 10. Examination of actinotrichia in fin sections following injection with standard control MO at different timepoints. Single plane confocal sections were obtained for longitudinal and transverse sections immunostained with Collagen type II (green) and counterstained with propidium iodide (red). Untreated fins are labeled as 'WT-5 dpa'. Longitudinal (top) and transverse (bottom) sections show regeneration of actinotrichia at different time points following injection and electroporation with standard control MO. Arrows indicate actinotrichia, 'e' is epidermis and 'm' mesenchyme. Scale bar is 10 μ m and applies to all panels.

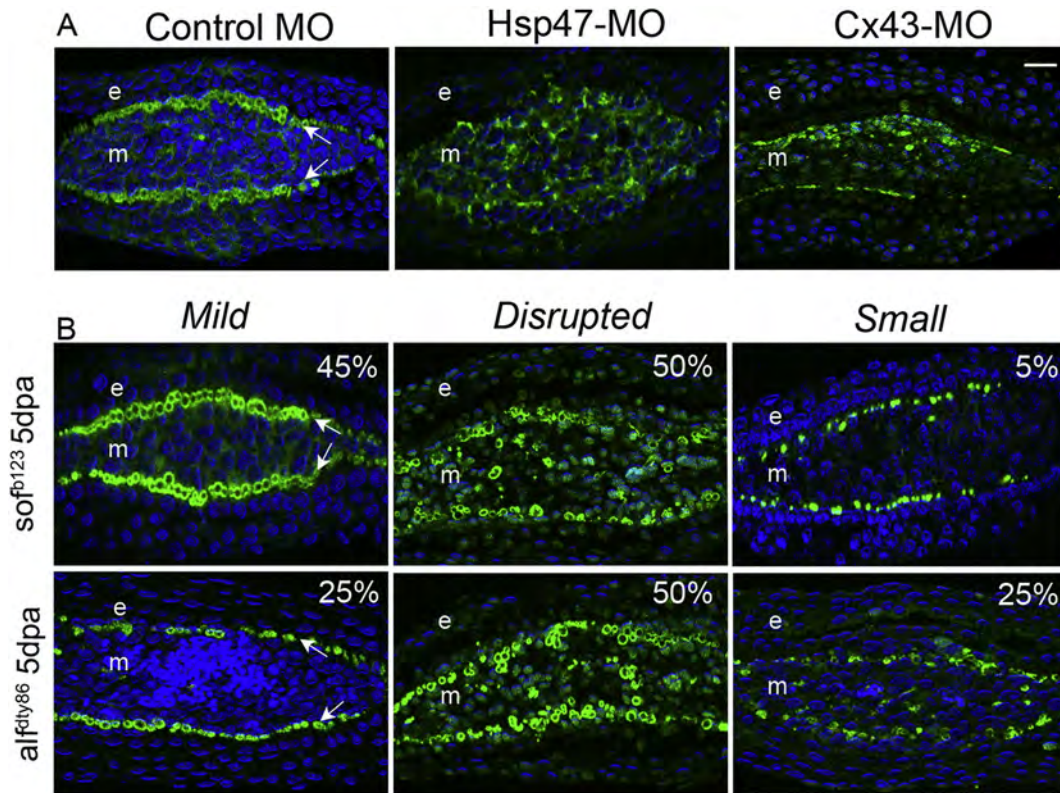


Fig. 11. Disruption of actinotrichia following changes in Hsp47 or Cx43 expression. Single plane confocal sections are obtained for transverse sections immunostained with Collagen type II (green) and counterstained for nuclei with To-pro (blue). (A) Fins are injected with standard control MO, Hsp47-MO or Cx43-MO and evaluated at 1 dpe. Col II expression is disrupted following Hsp47 and Cx43 knockdown. (B) Variable actinotrichia phenotypes observed in 5 dpa transverse sections of both *sof^{b123}* and *alf^{dy86}*. The defects were categorized as mild, disrupted organization, or small. Arrows indicate actinotrichia, 'e' is epidermis and 'm' mesenchyme. Scale bar is 10 μm and applies to all panels.

10 min at 4 °C. The protein concentration in the supernatant was analyzed using a Bradford assay.

Immunoblotting was performed using previously described procedure (Hoptak-Solga et al., 2008). The following primary antibodies were used: Rabbit anti-Hsp47 (Abcam, 1:1000), Mouse anti- α -tubulin (Sigma, 1:2000). The following peroxidase conjugated secondary antibodies were used: Goat anti-rabbit IgG (1:10,000) and Goat anti-mouse IgG (1:10,000). Signal detection was performed using ECL Prime western blotting detection reagent (Amersham™ – GE Healthcare).

Relative pixel density of gel bands were measured using gel analysis tool in ImageJ software. The density of each gel band was obtained as the area under the curve using the gel analysis tool. In order to obtain the relative density, the density of the Hsp47 or tubulin bands for the

experimental samples (i.e. Hsp47 MO, *sof^{b123}* or *alf^{dy86}*) was first normalized against the density of the Hsp47 or tubulin bands from the control sample (i.e. standard control MO or WT). Relative pixel density was calculated as the ratio of Hsp47 and Tubulin (loading control).

4.6. Immunofluorescence

Fins were harvested following MO knockdown. For H3P staining, fins were harvested 1 dpe, whereas for ZNS5 staining, fins were harvested 4 dpe. They were then fixed in 4% paraformaldehyde (PFA) overnight at 4 °C and then dehydrated in methanol. H3P and ZNS5 staining were carried out following previously described procedures (Ton and Iovine, 2012). For calcein staining, MO injected fish were allowed to swim in 0.2% calcein solution (pH = 7) for 10 min, followed by

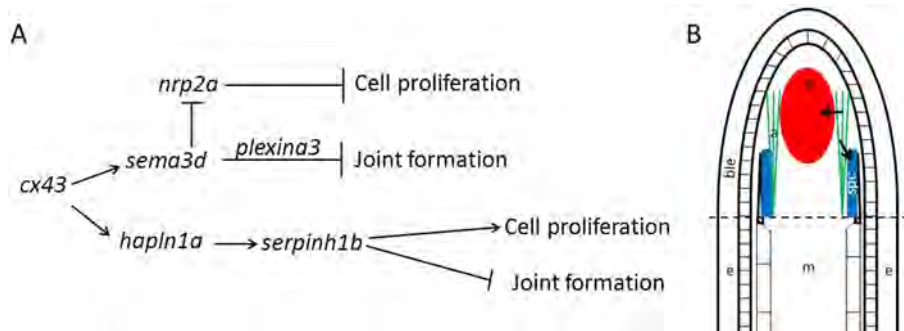


Fig. 12. Model for *serpinh1b* and Hsp47 in regeneration. (A) Transcriptional network of *cx43*-dependent genes. The *sema3d* and *hapln1a* genes were shown to be transcriptionally regulated in independent *cx43* pathways (Ton and Iovine, 2012; Govindan and Iovine, 2014). The *serpinh1b* gene is placed downstream of *hapln1a* based on this study. (B) Speculative model for how Hsp47 may influence bone growth and patterning. Defective Hsp47 leads to disturbed collagen-based actinotrichia (green). Defects in collagen may signal to proliferating cells in the blastema (red) and to skeletal precursor cells (blue) in the lateral compartment. a, actinotrichia, b, blastema, ble, basal layer of the epidermis, m, mesenchyme, e, epidermis, spc, skeletal precursor cells. The dotted line represents the amputation plane.

additional 10 min in fresh fish water (Du et al., 2001). Fluorescent fins were examined under a Nikon Eclipse 80i microscope at 4× or 10× magnification. Images were collected using a digital Nikon camera.

4.7. Measurement

The regenerate length, segment length and number of dividing cells were calculated as previously described (Ton and Iovine, 2012). In brief, for regenerate length, segment length, number of dividing cells and regenerated bone matrix, all measurements were taken from the third fin ray. Regenerate length was measured from the amputation plane to the end of the fin. Segment length was measured as the distance between the first two joints formed following amputation. For regenerating bone matrix, bone growth was measured from the amputation plane to the distal tip of the calcein stained bone matrix and was divided by the total regenerate length. H3P positive cells were counted from within the distal-most 250 μm of the third fin ray. For each experiment, at least seven fish were evaluated in triplicate and a Student's *t*-test was performed to indicate statistical significance ($p < 0.05$). In order to evaluate the phenotypic effect following knockdown of Hsp47, the targeting or the control MO injected side was compared with the uninjected side and % similarity was calculated by dividing the value of injected side by uninjected side and multiplying by 100. Values close to 100% indicate no effect of the MO on the injected side, whereas values different from 100% indicate that the MO had an effect on injected side. Percent similarity of greater than 100% reflects the fact that the experimental side can be measurably larger than the control uninjected side. Statistical significance was determined using Student's *t*-test ($p < 0.05$).

4.8. Quantitative real time PCR analysis

For qRT-PCR analysis, RNA was extracted using TRIZOL from 5 dpa fins for WT, *sof*^{b123} and *alf*^{dy86} and 1 dpe for MO injected fins (targeting or control). A minimum of eight fins were used for total RNA extraction and for each sample, 1 μg of RNA was reverse transcribed using Superscript III Reverse transcriptase (Invitrogen) and oligo-dT primers. Primers for *serpinh1b*, *msxc* and *mps1* were designed using Primer express software (Table 1). For *msxb*, we used the primer sequence from Kizil et al. (2009). Three independent RNA samples were used for each experiment, and each reaction was performed in duplicate. The samples were analyzed using Rotor Gene 6000 series software (Corbett Research) and the average cycle number (C_T) was calculated for each amplicon. Samples were then normalized with respect to the housekeeping gene *keratin* (Sims et al., 2009), and ΔC_T values were obtained. The relative level of gene expression or 'fold difference' was denoted by calculating $2^{-\Delta\Delta C_T}$. To obtain a range over which the fold-difference varies, we calculated a standard deviation for the $\Delta\Delta C_T$ values. We used the high and low $\Delta\Delta C_T$ values to calculate the high and low fold-difference values. When these values span a fold-difference of 1, it is interpreted as no change in expression from the control sample.

4.9. Immunofluorescence on sections

Fins were harvested at different timepoints following injections and fixed in 2% PFA for 30 min at room temperature. They were then washed in 1× PBS (3×, 5 min each), embedded in 1.5% agarose/5% sucrose dissolved in 1× PBS and equilibrated in 30% sucrose solution overnight. Fins were mounted in OCT and cryosectioned (18 μm) using a Reichert Jung 2800 Frigocut cryostat. Sections were collected on Superfrost Plus slides (Fisher) and allowed to air dry overnight at room temperature. Sections were stored in −20 °C for future use. Before use, slides were brought to room temperature for an hour, then rehydrated in 1× PBS (2×, 5 min each). They were then transferred to coplin jars containing 10 mM sodium citrate (pH = 6) and allowed to boil at 99.5 °C in the

water bath for 10 min. The slides were allowed to cool down to room temperature and again washed in 1× PBS (2×, 5 min each). Permeabilization was achieved by treating the slides with 1% H₂O₂ solution in water for 20 min at room temperature followed by 2× wash in 1× PBS for five minutes each. The slides were then transferred to block (2% BSA, 0.1% Triton-X in 1× PBS). Two quick washes in block (10 min each) were followed by an hour of incubation in block. The following primary antibodies were used: Rabbit anti-Hsp47 (Abcam, 1:100), Mouse anti-collagen type II (DSHB-II-II6B3, 1:10). Sections were circled using a PAP pen (Fisher or VWR laboratories). The slides were incubated in primary antibody overnight at 4 °C in a wet box followed by one quick wash and three 10 min washes in block. The following secondary antibodies were used: Anti-rabbit Alexa Fluor 488 or 568 (1:200), Anti-mouse Alexa Fluor 488 or 568 (1:200). Propidium iodide or To-Pro-3-iodide (Life Technologies, 1:1000) was used to stain the nuclei. The slides were incubated with secondary antibody for either an hour at room temperature or overnight at 4 °C, protected from light. It was followed by three 15 min washes in block and one quick wash in distilled water. They were then mounted with Glycerol or Vectashield and were examined under LSM 510 Meta Confocal Microscope (Zeiss) at 40×, using Argon (488) and HeNe (543 and 633) lasers. Z-stacks were collected with a depth of 0.36 μm.

Supplementary data to this article can be found online at <http://dx.doi.org/10.1016/j.mod.2015.06.004>.

Acknowledgments

The authors wish to thank Rebecca Bowman for care of the zebrafish colony, and members of the Iovine lab for critical evaluation of this manuscript. The ZNS5 antibody was obtained through the Zebrafish International Resource Center (supported by grant P40 RR12546 from the NIH-NCRR). The Col II antibody (II-II6B3) developed by Linsenmayer, T.F. was obtained from the Developmental Studies Hybridoma Bank, created by the NICHD of the NIH and maintained at The University of Iowa, Department of Biology, Iowa City, IA 52242. This work was supported by the NSF (IOS-1145582).

References

- Akimenko, M.A., Johnson, S.L., Westerfield, M., Ekker, M., 1995. Differential induction of four *msx* homeobox genes during fin development and regeneration in zebrafish. *Development* 121, 347–357.
- Christiansen, H.E., Schwarze, U., Pyott, S.M., AlSwaid, A., Al Balwi, M., Alrasheed, S., Pepin, M.G., Weis, M.A., Eyre, D.R., Byers, P.H., 2010. Homozygosity for a missense mutation in SERPINH1, which encodes the collagen chaperone protein HSP47, results in severe recessive osteogenesis imperfecta. *Am. J. Hum. Genet.* 86, 389–398.
- Diab, M., Wu, J.J., Eyre, D.R., 1996. Collagen type IX from human cartilage: a structural profile of intermolecular cross-linking sites. *Biochem. J.* 314 (Pt 1), 327–332.
- Du, S.J., Frenkel, V., Kindschi, G., Zohar, Y., 2001. Visualizing normal and defective bone development in zebrafish embryos using the fluorescent chromophore calcein. *Dev. Biol.* 238, 239–246.
- Duran, I., Mari-Beffa, M., Santamaria, J.A., Becerra, J., Santos-Ruiz, L., 2011. Actinotrichia collagens and their role in fin formation. *Dev. Biol.* 354, 160–172.
- Eyre, D.R., Weis, M.A., 2013. Bone collagen: new clues to its mineralization mechanism from recessive osteogenesis imperfecta. *Calcif. Tissue Int.* 93, 338–347.
- Fisher, S., Jagadeeswaran, P., Halpern, M.E., 2003. Radiographic analysis of zebrafish skeletal defects. *Dev. Biol.* 264, 64–76.
- FleNNiken, A.M., Osborne, L.R., Anderson, N., Ciliberti, N., Fleming, C., Gittens, J.E., Gong, X.Q., Kelsey, L.B., Lounsbury, C., Moreno, L., Nieman, B.J., Peterson, K., Qu, D., Roscoe, W., Shao, Q., Tong, D., Veitch, G.I., Voronina, I., Vukobradovic, I., Wood, G.A., Zhu, Y., Zirngibl, R.A., Aubin, J.E., Bai, D., Bruneau, B.G., Grynepas, M., Henderson, J.E., Henkelman, R.M., McKerlie, C., Sled, J.G., Stanford, W.L., Laird, D.W., Kidder, G.M., Adamson, S.L., Rossant, J., 2005. A Gja1 missense mutation in a mouse model of oculodentodigital dysplasia. *Development* 132, 4375–4386.
- Goodenough, D.A., Goliger, J.A., Paul, D.L., 1996. Connexins, connexons, and intercellular communication. *Annu. Rev. Biochem.* 65, 475–502.
- Govindan, J., Iovine, M.K., 2014. Hapln1a is required for connexin43-dependent growth and patterning in the regenerating fin skeleton. *PLoS One* 9, e88574.
- Heino, J., 2014. Cellular signaling by collagen-binding integrins. *Adv. Exp. Med. Biol.* 819, 143–155.
- Hoptak-Solga, A.D., Nielsen, S., Jain, I., Thummel, R., Hyde, D.R., Iovine, M.K., 2008. Connexin43 (GJA1) is required in the population of dividing cells during fin regeneration. *Dev. Biol.* 317, 541–548.

- Huang, C.C., Wang, T.C., Lin, B.H., Wang, Y.W., Johnson, S.L., Yu, J., 2009. Collagen IX is required for the integrity of collagen II fibrils and the regulation of vascular plexus formation in zebrafish caudal fins. *Dev. Biol.* 332, 360–370.
- Iovine, M.K., Higgins, E.P., Hindes, A., Coblitz, B., Johnson, S.L., 2005. Mutations in connexin43 (CJA1) perturb bone growth in zebrafish fins. *Dev. Biol.* 278, 208–219.
- Ishida, Y., Nagata, K., 2011. Hsp47 as a collagen-specific molecular chaperone. *Methods Enzymol.* 499, 167–182.
- Jones, S.J., Gray, C., Sakamaki, H., Arora, M., Boyde, A., Gourdie, R., Green, C., 1993. The incidence and size of gap junctions between the bone cells in rat calvaria. *Anat. Embryol. (Berl.)* 187, 343–352.
- Kizil, C., Otto, G.W., Geisler, R., Nusslein-Volhard, C., Antos, C.L., 2009. Simplex controls cell proliferation and gene transcription during zebrafish caudal fin regeneration. *Dev. Biol.* 325, 329–340.
- Lecanda, F., Warlow, P.M., Sheikh, S., Furlan, F., Steinberg, T.H., Civitelli, R., 2000. Connexin43 deficiency causes delayed ossification, craniofacial abnormalities, and osteoblast dysfunction. *J. Cell Biol.* 151, 931–944.
- Lee, Y., Grill, S., Sanchez, A., Murphy-Ryan, M., Poss, K.D., 2005. Fgf signaling instructs position-dependent growth rate during zebrafish fin regeneration. *Development* 132, 5173–5183.
- Masago, Y., Hosoya, A., Kawasaki, K., Kawano, S., Nasu, A., Toguchida, J., Fujita, K., Nakamura, H., Kondoh, G., Nagata, K., 2012. The molecular chaperone Hsp47 is essential for cartilage and endochondral bone formation. *J. Cell Sci.* 125, 1118–1128.
- McConnell, I.M., Green, C.R., Tickle, C., Becker, D.L., 2001. Connexin43 gap junction protein plays an essential role in morphogenesis of the embryonic chick face. *Dev. Dyn.* 222, 420–438.
- Nagai, N., Hosokawa, M., Itohara, S., Adachi, E., Matsushita, T., Hosokawa, N., Nagata, K., 2000. Embryonic lethality of molecular chaperone hsp47 knockout mice is associated with defects in collagen biosynthesis. *J. Cell Biol.* 150, 1499–1506.
- Nakai, A., Satoh, M., Hirayoshi, K., Nagata, K., 1992. Involvement of the stress protein HSP47 in procollagen processing in the endoplasmic reticulum. *J. Cell Biol.* 117, 903–914.
- Nechiporuk, A., Keating, M.T., 2002. A proliferation gradient between proximal and msxb-expressing distal blastema directs zebrafish fin regeneration. *Development* 129, 2607–2617.
- Paznekas, W.A., Karczeski, B., Vermeer, S., Lowry, R.B., Delatycki, M., Laurence, F., Koivisto, P.A., Van Maldergem, L., Boyadjiev, S.A., Bodurtha, J.N., Jabs, E.W., 2009. GJA1 mutations, variants, and connexin 43 dysfunction as it relates to the oculodentodigital dysplasia phenotype. *Hum. Mutat.* 30, 724–733.
- Pearson, D.S., Kulyk, W.M., Kelly, G.M., Krone, P.H., 1996. Cloning and characterization of a cDNA encoding the collagen-binding stress protein hsp47 in zebrafish. *DNA Cell Biol.* 15, 263–272.
- Perathoner, S., Daane, J.M., Henrion, U., Seebohm, G., Higdon, C.W., Johnson, S.L., Nusslein-Volhard, C., Harris, M.P., 2014. Bioelectric signaling regulates size in zebrafish fins. *PLoS Genet.* 10, e1004080.
- Poss, K.D., Nechiporuk, A., Hillam, A.M., Johnson, S.L., Keating, M.T., 2002. Mps1 defines a proximal blastemal proliferative compartment essential for zebrafish fin regeneration. *Development* 129, 5141–5149.
- Quint, E., Smith, A., Avaron, F., Laforest, L., Miles, J., Gaffield, W., Akimenko, M.A., 2002. Bone patterning is altered in the regenerating zebrafish caudal fin after ectopic expression of sonic hedgehog and bmp2b or exposure to cyclopamine. *Proc. Natl. Acad. Sci. U. S. A.* 99, 8713–8718.
- Ramachandran, L.K., 1962. Elastoidin—a mixture of three proteins. *Biochem. Biophys. Res. Commun.* 6, 443–448.
- Reaume, A.G., de Sousa, P.A., Kulkarni, S., Langille, B.L., Zhu, D., Davies, T.C., Juneja, S.C., Kidder, G.M., Rossant, J., 1995. Cardiac malformation in neonatal mice lacking connexin43. *Science* 267, 1831–1834.
- Sastry, L.V., Ramachandran, L.K., 1965. The protein components of elastoidin. *Biochim. Biophys. Acta* 97, 281–287.
- Satoh, M., Hirayoshi, K., Yokota, S., Hosokawa, N., Nagata, K., 1996. Intracellular interaction of collagen-specific stress protein HSP47 with newly synthesized procollagen. *J. Cell Biol.* 133, 469–483.
- Sims Jr., K., Eble, D.M., Iovine, M.K., 2009. Connexin43 regulates joint location in zebrafish fins. *Dev. Biol.* 327, 410–418.
- Smith, A., Avaron, F., Guay, D., Padhi, B.K., Akimenko, M.A., 2006. Inhibition of BMP signaling during zebrafish fin regeneration disrupts fin growth and scleroblast differentiation and function. *Dev. Biol.* 299, 438–454.
- Sohl, G., Willecke, K., 2004. Gap junctions and the connexin protein family. *Cardiovasc. Res.* 62, 228–232.
- Thummel, R., Bai, S., Sarras Jr., M.P., Song, P., McDermott, J., Brewer, J., Perry, M., Zhang, X., Hyde, D.R., Godwin, A.R., 2006. Inhibition of zebrafish fin regeneration using in vivo electroporation of morpholinos against fgfr1 and msxb. *Dev. Dyn.* 235, 336–346.
- Ton, Q.V., Iovine, M.K., 2012. Semaphorin3d mediates Cx43-dependent phenotypes during fin regeneration. *Dev. Biol.* 366, 195–203.
- Ton, Q.V., Iovine, M.K., 2013. Identification of an evx1-dependent joint-formation pathway during FIN regeneration. *PLoS One* 8, e81240.
- van Eeden, F.J., Granato, M., Schach, U., Brand, M., Furutani-Seiki, M., Haffter, P., Hammerschmidt, M., Heisenberg, C.P., Jiang, Y.J., Kane, D.A., Kelsh, R.N., Mullins, M.C., Odenthal, J., Warga, R.M., Nusslein-Volhard, C., 1996. Genetic analysis of fin formation in the zebrafish, *Danio rerio*. *Development* 123, 255–262.
- Westerfield, M., 1993. *The Zebrafish Book: A Guide for the Laboratory Use of Zebrafish (Brachydanio rerio)*. University of Oregon Press, Eugene, OR.
- Widmer, C., Gebauer, J.M., Brunstein, E., Rosenbaum, S., Zaucke, F., Drogemuller, C., Leeb, T., Baumann, U., 2012. Molecular basis for the action of the collagen-specific chaperone Hsp47/SERPINH1 and its structure-specific client recognition. *Proc. Natl. Acad. Sci. U. S. A.* 109, 13243–13247.
- Wood, A., 1982. Early pectoral fin development and morphogenesis of the apical ectodermal ridge in the killifish, *Aphyosemion scheeli*. *Anat. Rec.* 204, 349–356.
- Zhang, J., Wagh, P., Guay, D., Sanchez-Pulido, L., Padhi, B.K., Korzh, V., Andrade-Navarro, M.A., Akimenko, M.A., 2010. Loss of fish actinotrichia proteins and the fin-to-limb transition. *Nature* 466, 234–237.